



COB-2021-1146

THEORETICAL ANALYSIS OF THE RAPID SOLIDIFICATION OF METALLIC MATERIALS IN PLANAR FLOW CASTING PROCESS THROUGH OF GENERALIZED INTEGRAL TRANSFORM TECHNIQUE

Marinaldo José de Medeiros

Federal University of Paraíba - Technology Center, Mechanical Engineering Graduate Program (PPGEM), Campus I, Cidade Universitária, Zip Code: 58.051-900, João Pessoa, Paraíba, Brazil, Phone: +55 83 3216-7186

Federal Institute of Paraíba - Campus Itabaiana
marinaldo.medeiros@ifpb.edu.br

Carlos Antonio Cabral dos Santos

Federal University of Paraíba - Technology Center- Department of Mechanical Engineering, Campus I, Cidade Universitária, Zip Code: 58.051-900, João Pessoa, Paraíba, Brazil, Phone: +55 83 3216-7356

carloscabraldosantos@yahoo.com.br

Abstract. *The Planar Flow Casting (PFC) is a single-stage fast solidification technique for the production of thin metallic ribbons. The objective of this research is to develop a mathematical model to analyze the phenomenon of heat transfer and phase change during the formation of the puddle, to determine the position of the interface and the temperature profile. The applied methodology consists of the use of the energy balance, where the equations of the energy (liquid and solid phases), and the equation of the interface are transformed through the Generalized Integral Transform Technique (GITT) being solved by the NDSolve routine of the Mathematica. This tool was capable to solve problem, can study the fast cooling of metals and obtain ribbons of thickness controlled by the speed of the wheel and for the heat transfer coefficient. Considering that the height of the puddle is very small and the process time is very short, a large number of eigenvalues used to obtain the convergence of the solution. The results of the temperature distribution along the length of the puddle and the evolution of the solidification front was compared with existing results in the literature, obtaining an adjustment of the order of 2 %.*

Keywords: *Moving Boundary, Planar Flow Casting, Generalized Integral Transform Technique.*

1. INTRODUCTION

Transient phase change problems involve the path followed by a movement of the solidification front, separating the liquid and solid phases of a substance. Inside of the liquid phase and the solid phase the process of transfer of heat is governed mainly by conduction.

The Planar Flow Casting (PFC) is a complicated solidification process, where heat and mass transfer, multiphase fluid flow and solidification occur concurrently. During the PFC process, molten alloy is continuously deposited onto a substrate of a cooling wheel through a nozzle slot. Upon contacting the substrate of cooling wheel, the molten alloy rapidly solidified and continuous ribbon is peeled off from the wheel and coiled by a winding machine.

The temper starting from the liquid metal is a process of rapid solidification that involves the shock with spreading and appearance of the solidification starting from the puddle of liquid metal on the surface of a substrate. Contrary to the traditional process of production, where the temper is made on sample of solid material, the rapid cooling starting from the liquid metal represents a separate category from temper in that the initial state of the metal is liquid (Jones, 1984; Annavarapu *et al.*, 1990).

This leads to a characteristic definition of the method of rapid cooling starting with the liquid metal, which is imposed by the speeds of cooling of the liquid metal, that are typically much faster than the conventional methods of temper. This situation happens when the heat transfer mechanism, mainly conduction, is capable of removing much faster the heat that comes out of the deposition layer than the heat that is deposited by the liquid metal. The fluid dynamics of the rapid solidification processes have also been the focus of many studies, the effects of heat transfer and phase change in planar flow casting processes was studied numerically by Wang and Matthys (1991, 1992); Carpenter and Steen (1992). Liu *et al.* (1993) investigated numerically the substrate impact and freezing of molten droplets in plasma spray processes.

Since the 90s, the industry has been showing interest in the technology of fast solidification of metals and alloys starting from the liquid state, because of its compact form and production capacity with fast performance, as well as

an improvement of the properties of the materials. Carpenter and Steen (1997) and Steen and Karcher (1997) provide a review of the fluid mechanics of the PFC process. Numerous studies have investigated the influences of casting parameters and casting conditions on the uniformity of ribbon thickness and the surface quality of peeled ribbon (Wang and Prasad, 2000; Wang and Matthys, 2001; Nascimento, 2002; Busmann *et al.*, 2002; Napolitano and Meco, 2004). Byrne *et al.* (2006) investigate the capillary puddle vibration on casting defect of ribbons in PFC process. Wang *et al.* (2010) studied the thermal and mechanical behavior of the solidifying shell during continuous steel casting. Liu *et al.* (2009a,b, 2010); Cox (2011); Swaroopa *et al.* (2015); Su *et al.* (2015, 2016) studied the dependence of ribbon thickness on the main process parameters and to developed a simple formulation that predicts the ribbon thickness in gap controlled PFC process. (Li *et al.*, 2017; Swaroopa *et al.*, 2017). Mattson *et al.* (2018); Mattson (2019) studied crystalline and non-crystalline alloys using the PFC process and it was found that the tape thickness depends on the thermal properties of the alloy and the heat transfer characteristics of the machine used to produce the tape. (Mu *et al.*, 2020; Li and Lu, 2020; Madireddi, 2020; Theisen and Weinstein, 2021) reviewed how PFC processes were developed, examined the typical operability range of PFC, and reviewed the defects that commonly form.

The main objective of this article is through mathematical model proposed analyze the phenomenon of heat transfer and phase change to determine the position of the interface and the temperature field to obtain well-finished metallic tapes or alloys with excellent properties through the application of Generalized Integral Transformation Technique (GITT) varying the heat transfer coefficient and using a constant uniform velocity flywheel already known in the literature, obtaining good results in comparison with the literature.

2. PLANAR FLOW CASTING PROCESS

The Planar Flow Casting (PFC) is a single-stage fast solidification technique for the production of thin metallic ribbons where the liquid metal in the crucible is forced through the hole and it forms the solidification puddle between the base of the crucible and the surface of wheel. The ribbon is dragged out of the melt puddle by the relative substrate motion depending on the heat transfer, nucleation and crystal growth characteristics, conform show in Fig. 1

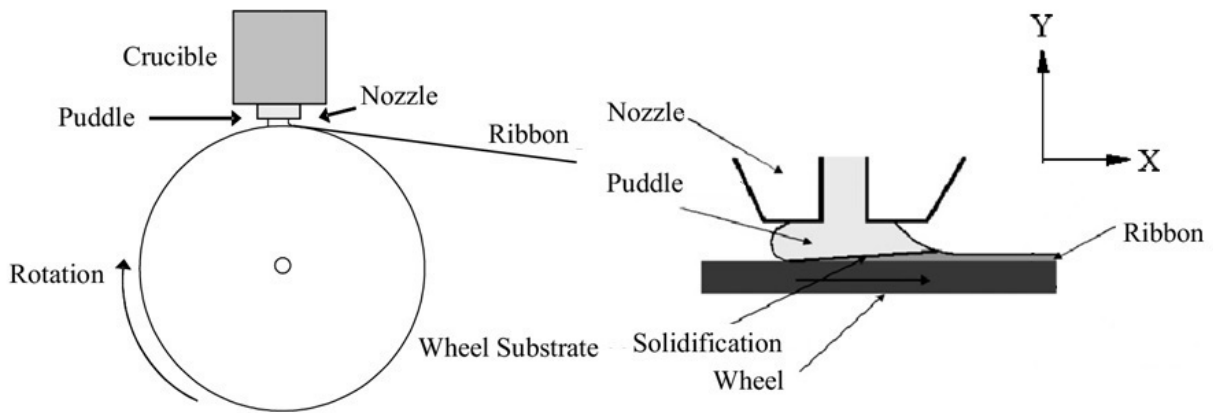


Figure 1. Schematic Diagram of the PFC Geometry used in Model

With the objective of making the model as simple as possible, let us consider that gradient of speed doesn't exist in the puddle. In fact, this is not true and it represents an approximation of a real case. To identify relative tendencies and to investigate important parameters in the process, we will adopt a one-dimensional model (Wang and Matthys, 1991, 1992), where the main simplifying hypotheses adapted were: Laminar flow; steady state; local thermodynamic equilibrium in the interface solid/liquid and constant specific mass for both phases.

With the assumptions considered above and assuming that a thin, immobile layer of liquid metal is suddenly brought into contact with the cooling substrate, in a very short period of time, then the liquid metal solidifies. If there is no relative movement between the fluid flow and the wheel, and if the deposited metallic layer (puddle) is thin, and also, due to the decoupling between the heat transfer process and the mechanics of the fluid flow, caused by the high speed of the substrate, we can approximate the heat transfer in the deposited metallic layer and in the substrate, with only one-dimensional conduction. Then, the energy equations for the boundary layer in each region are given, such as:

Solid Region:

$$V_w \frac{\partial T_S(y,t)}{\partial x} = \alpha_s \frac{\partial^2 T_S(y,t)}{\partial y^2} ; 0 < y < S(t) ; t > t_0 \quad (1)$$

Liquid Region:

$$V_w \frac{\partial T_L(y, t)}{\partial x} = \alpha_L \frac{\partial^2 T_L(y, t)}{\partial y^2} ; S(t) < y < L ; t > t_0 \quad (2)$$

Interface:

$$K_s \frac{\partial T_S(y, t)}{\partial y} - K_L \frac{\partial T_L(y, t)}{\partial y} = \rho \Delta H \frac{\partial S(t)}{\partial t} ; y = S(t) ; t > t_0 \quad (3)$$

and boundary conditions:

$$K_S \frac{\partial T_S(y, t)}{\partial y} = h_w (T_S - T_\infty) ; y = 0 ; t > t_0 \quad (4)$$

$$T_S = T_L = T_\infty ; y = S(t) ; t > t_0 \quad (5)$$

$$T_L = T_0 ; y = 0, t > t_0, \quad (6)$$

The solid and liquid region and interface equation can also be rewritten after introducing the following dimensionless groups:

$$\eta_1 = \frac{y}{S(t)} ; \eta_2 = \frac{y - L}{S(t) - L} ; Bi = \frac{h_w L}{K_S} ; \nu = \sqrt{\frac{\alpha_L}{\alpha_S}} ; S(\tau) = \frac{S(t)}{L} ; \tau = \frac{\alpha_L t}{L^2} \quad (7)$$

$$\theta_S(\eta_1, \tau) = \frac{T_S - T_\infty}{T_m - T_\infty} ; \theta_L(\eta_2, \tau) = \frac{T_L - T_0}{T_m - T_0} ; Ste_L = \frac{CP_L(T_m - T_0)}{\Delta H} ; Ste_S = \frac{CP_S(T_m - T_\infty)}{\Delta H} \quad (8)$$

and introduce a domain regularization transformation for the spatial domain written:

$$\frac{\partial}{\partial y} = \frac{\partial}{\partial \eta_i} \frac{\partial \eta_i}{\partial y} , \quad \frac{\partial}{\partial t} = \frac{\partial}{\partial \tau} \frac{\partial \tau}{\partial t} + \frac{\partial}{\partial \eta_i} \frac{\partial \eta_i}{\partial \tau} \text{ for } i = 1(\text{solid}) \text{ and } i = 2(\text{liquid}) \quad (9)$$

Then, the dimensionless form for solid and liquid region and interface equations after the domain transformation for the spatial domain written as:

Solid Region:

$$\frac{\partial \theta_S}{\partial \tau} = \frac{1}{\nu^2 S(\tau)^2} \frac{\partial^2 \theta_S}{\partial \eta_1^2} + \eta_1 \frac{S'(\tau)}{S(\tau)} \frac{\partial \theta_S}{\partial \eta_1} ; 0 < \eta_1 < 1 ; \tau > \tau_0, \quad (10)$$

Liquid Region

$$\frac{\partial \theta_L}{\partial \tau} = \frac{1}{(S(\tau) - 1)^2} \frac{\partial^2 \theta_L}{\partial \eta_2^2} + \frac{S'(\tau)}{(S(\tau) - 1)} \eta_2 \frac{\partial \theta_L}{\partial \eta_2} ; 0 < \eta_2 < 1 ; \tau > \tau_0 \quad (11)$$

Interface

$$\frac{dS(\tau)}{d\tau} = \frac{Ste_S}{\nu^2 S(\tau)} \frac{\partial \theta_S}{\partial \eta_1} \Big|_{\eta_1=1} - \frac{Ste_L}{(S(\tau) - 1)} \frac{\partial \theta_L}{\partial \eta_2} \Big|_{\eta_2=1} \quad (12)$$

and boundary conditions:

$$-\frac{\partial \theta_S(0, \tau)}{\partial \eta_1} + Bi S(\tau) \theta_S(0, \tau) = 0 ; \tau > \tau_0 \quad (13)$$

$$\theta_S(1, \tau) = 1 ; \theta_L(1, \tau) = 1 ; \tau > \tau_0 \quad (14)$$

$$\theta_L(0, \tau) = 0 ; \tau > \tau_0, \quad (15)$$

3. METHODOLOGY

With the objective of improving the performance of GITT, it is necessary to homogenize the boundary conditions of problem

$$\theta_S(\eta_1, \tau) = F_S(\eta_1; \tau) + \phi_S(\eta_1, \tau) ; \theta_L(\eta_2, \tau) = F_L(\eta_2; \tau) + \phi_L(\eta_2, \tau) \quad (16)$$

The solutions to the filter equations are given by:

$$F_S(\eta_1; \tau) = \frac{BiS(\tau)\eta_1 + 1}{1 + BiS(\tau)} = f(\tau) ; F_L(\eta_2; \tau) = \eta_2, \quad (17)$$

Inserting the filters in the solid and liquid region and interface equations, we obtain:

$$\frac{\partial \phi_S}{\partial \tau} = \frac{1}{\nu^2 S(\tau)^2} \frac{\partial^2 \phi_S}{\partial \eta_1^2} + \eta_1 \frac{S'(\tau)}{S(\tau)} \left(\frac{\partial \phi_S}{\partial \eta_1} + f(\tau) \right) - f'(\tau) ; 0 < \eta_1 < 1 ; \tau > \tau_0 \quad (18)$$

$$\frac{\partial \phi_L}{\partial \tau} = \frac{1}{(S(\tau) - 1)^2} \frac{\partial^2 \phi_L}{\partial \eta_2^2} + \eta_2 \frac{S'(\tau)}{(S(\tau) - 1)} \left(\frac{\partial \phi_L}{\partial \eta_2} + 1 \right) ; 0 < \eta_2 < 1 ; \tau > \tau_0 \quad (19)$$

$$\frac{dS(\tau)}{d\tau} = \frac{Ste_S}{\nu^2 S(\tau)} \left(\frac{\partial \phi_S}{\partial \eta_1} + \frac{BiS(\tau)}{1 + BiS(\tau)} \right) \Big|_{\eta_1=1} - \frac{Ste_L}{(S(\tau) - 1)} \left(\frac{\partial \phi_L}{\partial \eta_2} + 1 \right) \Big|_{\eta_2=1} ; \tau > \tau_0, \quad (20)$$

Following the basic steps of GITT, (Cotta, 2020), the appropriate auxiliary problems for the process of integral transform, are given as follows:

Solid Region

$$\frac{d^2 \psi(\eta_1)}{d\eta_1^2} + \mu_i^2 \psi(\eta_1) = 0 ; -\frac{d\psi(0)}{d\eta_1} + BiS(\tau)\psi(0) = 0 ; \psi(1) = 0 \quad (21)$$

which is readily solved eigenfunctions, normalized eigenfunctions, eigenvalues and norms, respectively, as:

$$\psi(\eta_1) = \text{Sin}[\mu_i(1 - \eta_1)] ; \tilde{\psi}(\eta_1) = \frac{\psi(\eta_1)}{\sqrt{N_i}} ; \mu_i \text{Cos}[\mu_i] = BiS(\tau) \text{Sin}[\mu_i] \quad (22)$$

$$N_i = \int_0^1 \psi_i(\eta_1) \psi_i(\eta_1) d\eta_1 = \frac{(BiS(\tau))^2 + BiS(\tau) + \mu_i^2}{2((BiS(\tau))^2 + \mu_i^2)} \quad (23)$$

Liquid Region

$$\frac{d^2 \chi(\eta_2)}{d\eta_2^2} + \xi_i^2 \chi(\eta_2) = 0 ; \chi(0) = 0 ; \chi(1) = 0 \quad (24)$$

which is readily solved eigenfunctions, normalized eigenfunctions, eigenvalues and norms, respectively, as:

$$\chi(\eta_2) = \text{Sin}[\xi_i \eta_2] ; \tilde{\chi}(\eta_2) = \frac{\chi(\eta_2)}{\sqrt{M_i}} ; \xi_i = i\pi \quad (25)$$

$$M_i = \int_0^1 \psi_i(\eta_1) \psi_i(\eta_1) d\eta_1 = \frac{1}{2} \quad (26)$$

The eigenvalue problems Eqs. (21) and (24) allows definition of the following transform-inverse pairs:

$$\overline{\phi_{S_j}}(\tau) = \int_0^1 \tilde{\psi}_j(\eta_1) \phi_S(\eta_1, \tau) d\eta_1 \rightarrow \text{Transform} \quad (27)$$

$$\phi_S(\eta_1, \tau) = \sum_{j=1}^{\infty} \tilde{\psi}_j(\eta_1) \overline{\phi_{S_j}}(\tau) \rightarrow \text{Inverse} \quad (28)$$

$$\overline{\phi_{L_j}}(\tau) = \int_0^1 \tilde{\chi}_j(\eta_2) \phi_L(\eta_2, \tau) d\eta_2 \rightarrow \text{Transform} \quad (29)$$

$$\phi_L(\eta_2, \tau) = \sum_{j=1}^{\infty} \tilde{\chi}_j(\eta_2) \overline{\phi_{L_j}}(\tau) \rightarrow \text{Inverse} \quad (30)$$

Applying the operators over Eqs. (17) and (19), followed by the inverse formula then results:

$$\frac{d\overline{\phi_{S_j}}(\tau)}{d\tau} = -\frac{\mu_i^2 \overline{\phi_{S_j}}(\tau)}{\nu^2 S(\tau)^2} + \frac{S'(\tau)}{S(\tau)} \sum_{j=1}^{\infty} A_{ij} \overline{\phi_{S_j}}(\tau) + \frac{S'(\tau)}{S(\tau)} B_i - \frac{S'(\tau)}{(1 + BiS(\tau))^2} B_i g_i \quad (31)$$

$$\frac{d\overline{\phi_{L_j}}(\tau)}{d\tau} = -\frac{\xi_i^2 \overline{\phi_{L_j}}(\tau)}{(S(\tau) - 1)^2} + \frac{S'(\tau)}{(S(\tau) - 1)} \sum_{j=1}^{\infty} C_{ij} \overline{\phi_{L_j}}(\tau) + \frac{S'(\tau)}{(S(\tau) - 1)} D_i \quad (32)$$

$$\frac{dS(\tau)}{d\tau} = \frac{Ste_S}{\nu^2 S(\tau)} \sum_{j=1}^{\infty} \left[\frac{d\psi_j(1)}{d\eta_1} \overline{\phi_{S_j}}(\tau) + \frac{BiS(\tau)}{1 + BiS(\tau)} \right] - \frac{Ste_L}{(S(\tau) - 1)} \sum_{j=1}^{\infty} \left[\frac{d\chi_j(1)}{d\eta_1} \overline{\phi_{L_j}}(\tau) + 1 \right] \quad (33)$$

with

$$A_{ij} = \int_0^1 \eta_1 \tilde{\psi}_i(\eta_1) \frac{d\tilde{\psi}_j(\eta_1)}{d\eta_1} d\eta_1 \quad (34)$$

$$B_i = \int_0^1 \eta_1 \tilde{\psi}_i(\eta_1) d\eta_1 \quad (35)$$

$$C_{ij} = \int_0^1 \eta_2 \tilde{\chi}_i(\eta_2) \frac{d\tilde{\chi}_j(\eta_2)}{d\eta_2} d\eta_2 \quad (36)$$

$$D_i = \int_0^1 \eta_2 \tilde{\chi}_i(\eta_2) d\eta_2 \quad (37)$$

$$g_i = \int_0^1 \psi_i(\eta_1) (1 - \eta_1) d\eta_1 \quad (38)$$

The initial conditions of the solid and liquid phases temperature field are transformed and written as:

$$\overline{\phi_{S_j}}(\tau_0) = \int_0^1 \tilde{\psi}_j(\eta_1) (\phi_{S_{Analit}}(\eta_1, \tau_0) - F_S(\eta_1, \tau_0)) d\eta_1 \quad (39)$$

$$\overline{\phi_{L_j}}(\tau_0) = \int_0^1 \tilde{\chi}_j(\eta_2) (\phi_{L_{Analit}}(\eta_2, \tau_0) - F_L(\eta_2, \tau_0)) d\eta_2 \quad (40)$$

Eqs. (31), (32) and (33) form an infinite system of one-dimensional partial differential equations for the transformed potentials. For computational purposes this system is truncated to a sufficient large finite order, NS and NL (liquid and solid region eigenvalues number), for the required convergence control. Once the transformed potentials are numerically computed, the inversion formula, Eqs. (28) and (30), is employed to reconstruct the filtered potentials, in explicit form in the transverse coordinate, and after adding the filtering solution, the dimensionless temperature distribution, is recovered everywhere within the region along the process.

4. RESULTS AND DISCUSSION

The simulation of the planar flow casting process provides the control and adjustment of the parameters involved in the production of metallic ribbons. The relation of those parameters with the heat transfer coefficients makes possible the adjustment of the process and use of different materials. The main parameters involved are: ejection temperature, distance from the crucible to the cooling substrate, substrate temperature, substrate speed, height and length of the puddle. For the conduct of the simulations, pure aluminum will be used, whose parameters involved in the solidification processes, have important influences in the monitoring of real and design processes.

In order to compare the results we extracted the properties obtained by Wang and Matthys (1992):

$$\Delta H = 3.95 \times 10^5 \text{ J/kg} ; CP_L = 1200 \text{ J/kgK} ; CP_S = 1060 \text{ J/kgK} ; V_w = 23 \text{ m/s} ; XD = 5,75 \text{ mm}$$

$$k_S = 200 \text{ W/mK} ; k_L = 100 \text{ W/mK} ; \rho = 2520 \text{ kg/m}^3 ; T_0 - T_m = 50 \text{ K} ; T_{\infty} = 300 \text{ K and .}$$

Fig. 2 shows the behavior of the temperature curves as a function of the distance to the upper meniscus, where solidification begins, for the aluminum metal on the copper flywheel. At the end of the process, the tape reached a thickness of $114 \mu\text{m}$, it can be seen that the temperature is above the solidification temperature, that is, at this thickness everything is liquid. As it moves in the vertical position (y) there is a phase change, in thickness $4 \mu\text{m}$ there is only solid, the position closer to the copper wheel. You can also see that as you move in the horizontal position (x), the temperature drops considerably, especially near the copper wheel. The lowest temperature reached was approximately 700 K due to the high heat transfer coefficient, whose adopted value was $h_w = 1.0 \times 10^6 \text{ W/m}^2 \text{ K}$.

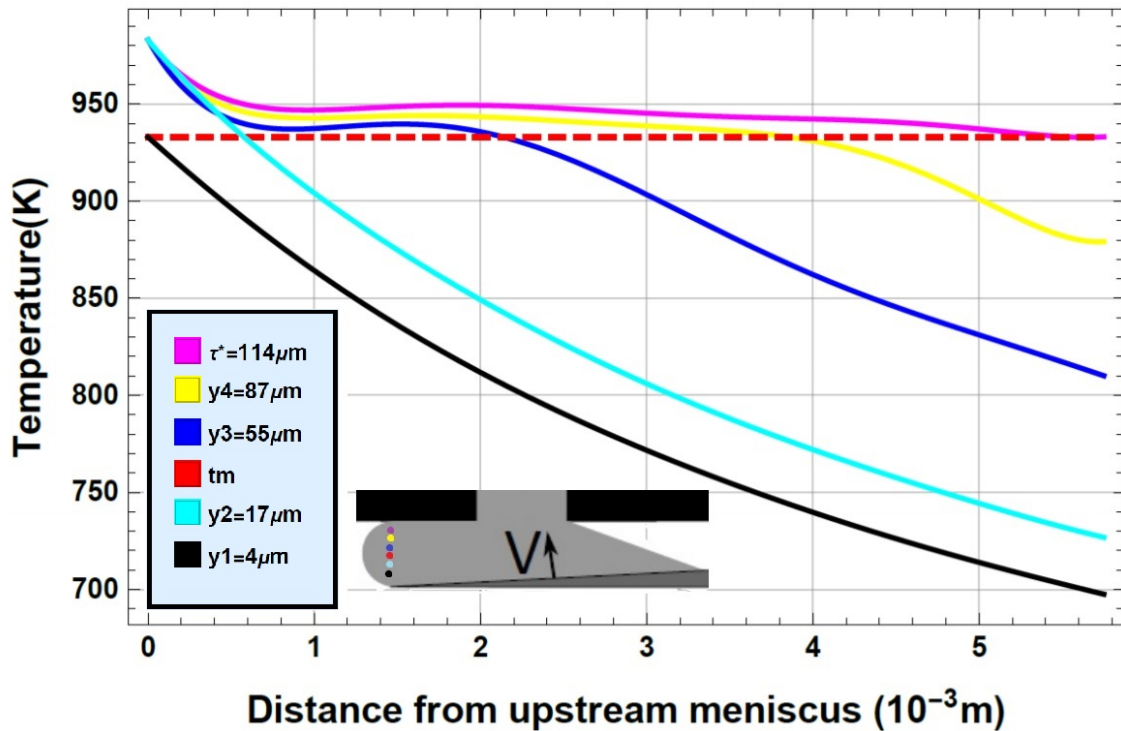


Figure 2. Temperature distribution as a function of the distance from upstream meniscus

The solidification front develops in relation to the position directions of x and y, according to the variables the process. In this situation, the inertia forces are much larger than the viscous forces of the fluid and the thickness of the ribbon is limited of the puddle the height of the solidification front, in the end of the length of the metal puddle.

Fig. 3 shows the evolution of the interface as a function of the point of start of solidification for the same metal during the process in Fig. 2. It is observed that the solidification frontier has an almost linear behavior, motivated by the short process time and the high speed of the flywheel.

In Tab. 1 shows the temperature distribution varying the distance of $21, 68$ and $114 \mu\text{m}$ from the base of the puddle, in the tape with a thickness equal to $114 \mu\text{m}$, it can be noted that as the distance from the base of the puddle decreases position of x (mm) for the 933 K temperature also decreases. In the distance of $114 \mu\text{m}$ only have liquid part because in the last position of $x = 5.75 \text{ mm}$ the temperature corresponds to 933 K , while in the distance of $21 \mu\text{m}$ have both liquid and solid part because the temperature of 933 K is in position $x = 0.575 \text{ mm}$.

In order to verify the influence of the heat transfer coefficient on the process, the following values were used:

$$h_w = 1.0 \times 10^6 \text{ W/m}^2 \text{ K} ; h_w = 2.0 \times 10^5 \text{ W/m}^2 \text{ K} \text{ and } h_w = 5.0 \times 10^5 \text{ W/m}^2 \text{ K}.$$

In Tab. 2 it can be seen that as we increase the number of eigenvalues, the temperature values started to converge in the fourth decimal place, this is due to the difficulty in determining the liquid / solid interface considering that the process time is very short. In addition, the height of the puddle is very small, so it is necessary to use many eigenvalues to achieve convergence.

In Fig. 4, as we increase the heat transfer coefficient, there is an increase in the evolution of the interface, this only corroborates with physical meaning because we are increasing the convection in the process. When comparing the solution obtained by the present work with the results obtained numerically by Wang and Matthys (1992), it can be seen that the curves are very close except for $h_w = 2.0 \times 10^5 \text{ W/m}^2 \text{ K}$, this is probably the limit for producing tapes with a good finish.

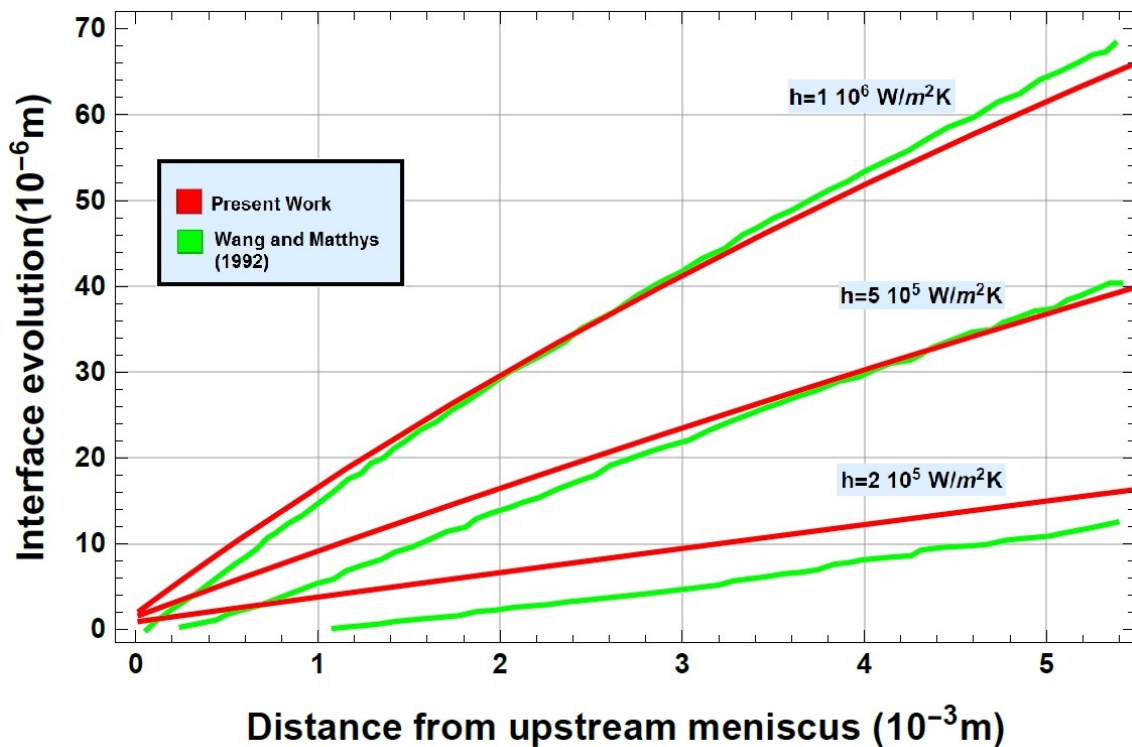


Figure 4. Interface evolution as a function of the distance from the upstream meniscus by varying the heat transfer coefficient

Comparing the results with the results obtained by Nascimento (2002), it can be observed that both present a good harmony with acceptable errors in the order of 1 % , which allows to prove that the model adopted using the NDSolve routine can be perfectly used. The drop in temperature as the metal approaches the copper wheel only corroborates the physical phenomenon, which corresponds to heat exchange by conduction, contributing to ensure that the use of the generalized integral transform technique presenting good harmony with results obtained experimentally in literature.

5. CONCLUSIONS

The Generalized Integral Transform Technique (GITT) was show a tool capable to solve the Planar Flow Casting Problem with that can study the fast solidification of metals or alloys and obtain ribbons of thickness controlled by the speed of the wheel and for the heat transfer coefficient. Considering that the height of the puddle is very small and the process time is very short, there is a need to use a large number of eigenvalues to obtain the convergence of the solution. The results of the temperature distribution along the length of the puddle and the evolution of the solidification front was compared with results obtained Wang and Matthys (1992); Nascimento (2002) presented excellent harmony. The solution for the representation of the Planar Flow Casting process allows the obtaining of results that can be used the engineering level. The influence of the parameters involved in the process and the relationship of these parameters with the heat transfer coefficient makes it possible to adjust the process and use different materials.

6. ACKNOWLEDGEMENTS

To the IFPB/Campus Itabaiana for the release of the teacher, to carry out the Doctorate, and PPGEM-UFPB for the financial support.

7. REFERENCES

- Annavarapu, S., Apelian, D. and Lawley, A., 1990. "Spray casting of steel strip: process analysis". *Metallurgical Transactions A*, Vol. 21, No. 12, pp. 3237–3256.
- Bussmann, M., Mostaghimi, J., Kirk, D. and Graydon, J., 2002. "A numerical study of steady flow and temperature fields within a melt spinning puddle". *International journal of heat and mass transfer*, Vol. 45, No. 19, pp. 3997–4010.
- Byrne, C.J., Theisen, E.A., Steen, P.H. and Reed, B.L., 2006. "Capillary puddle vibrations linked to casting-defect formation in planar-flow melt spinning". *Metallurgical and Materials Transactions B*, Vol. 37, No. 3, pp. 445–456.
- Carpenter, J. and Steen, P., 1992. "Planar-flow spin-casting of molten metals: process behaviour". *Journal of materials*

- science*, Vol. 27, No. 1, pp. 215–225.
- Carpenter, J. and Steen, P., 1997. “Heat transfer and solidification in planar-flow melt-spinning: high wheelspeeds”. *International journal of heat and mass transfer*, Vol. 40, No. 9, pp. 1993–2007.
- Cotta, R.M., 2020. *Integral transforms in computational heat and fluid flow*. CRC Press.
- Cox, B., 2011. “Planar-flow melt spinning: Process dynamics and defect formation”.
- Jones, H., 1984. “The status of rapid solidification of alloys in research and application”. *Journal of Materials Science*, Vol. 19, No. 4, pp. 1043–1076.
- Li, D. and Lu, Z., 2020. “The effects of aging on the cyclical thermal shock response of a copper-beryllium alloy as a substrate of cooling wheel in planar flow casting process”. *Materials Research Express*, Vol. 7, No. 11, p. 116511.
- Li, Z., Yao, K., Li, D., Ni, X. and Lu, Z., 2017. “Core loss analysis of finemet type nanocrystalline alloy ribbon with different thickness”. *Progress in Natural Science: Materials International*, Vol. 27, No. 5, pp. 588–592.
- Liu, H., Chen, W., Chen, Y. and Liu, G., 2010. “Thermal deformation analysis of the rotating roller in planar flow casting process”. *ISIJ international*, Vol. 50, No. 10, pp. 1431–1440.
- Liu, H., Chen, W. and Liu, G., 2009a. “Parametric investigation of interfacial heat transfer and behavior of the melt puddle in planar flow casting process by numerical simulation”. *ISIJ international*, Vol. 49, No. 12, pp. 1895–1901.
- Liu, H., Chen, W., Qiu, S. and Liu, G., 2009b. “Numerical simulation of initial development of fluid flow and heat transfer in planar flow casting process”. *Metallurgical and Materials Transactions B*, Vol. 40, No. 3, pp. 411–429.
- Liu, H., Lavernia, E.J. and Rangel, R.H., 1993. “Numerical simulation of substrate impact and freezing of droplets in plasma spray processes”. *Journal of Physics D: Applied Physics*, Vol. 26, No. 11, p. 1900.
- Madireddi, S., 2020. “Effect of heat transfer between melt puddle and cooling wheel on amorphous ribbon formation”. *Engineering Science and Technology, an International Journal*, Vol. 23, No. 5, pp. 1162–1170.
- Mattson, J., Theisen, E. and Steen, P., 2018. “Rapid solidification forming of glassy and crystalline ribbons by planar flow casting”. *Chemical Engineering Science*, Vol. 192, pp. 1198–1208.
- Mattson, J.W., 2019. “On the production of crystalline and noncrystalline metals via the planar flow casting process”.
- Mu, Y., Hang, L., Zhao, G., Wang, X., Zhou, Y. and Cheng, Z., 2020. “Modeling and simulation for the investigation of polymer film casting process using finite element method”. *Mathematics and Computers in Simulation*, Vol. 169, pp. 88–102.
- Napolitano, R.E. and Meco, H., 2004. “The role of melt pool behavior in free-jet melt spinning”. *Metallurgical and Materials Transactions A*, Vol. 35, No. 5, pp. 1539–1553.
- Nascimento, A.A., 2002. *Theoretical Study of the Solidification of Metal Materials in Rapid Cooling using the Generalized Integral Transform Technique (in Portuguese)*. Ph.D. thesis, Graduate Program in Mechanical Engineering, Federal University of Paraíba, João Pessoa, Brasil.
- Steen, P.H. and Karcher, C., 1997. “Fluid mechanics of spin casting of metals”. *Annual review of fluid mechanics*, Vol. 29, No. 1, pp. 373–397.
- Su, Y.G., Chen, F., Wu, C.Y. and Chang, M.H., 2016. “Effect of surface roughness of chill wheel on ribbon formation in the planar flow casting process”. *Journal of Materials Processing Technology*, Vol. 229, pp. 609–613.
- Su, Y.G., Chen, F., Wu, C.Y., Chang, M.H. and Chung, C.A., 2015. “Effects of manufacturing parameters in planar flow casting process on ribbon formation and puddle evolution of fe–si–b alloy”. *ISIJ International*, Vol. 55, No. 11, pp. 2383–2390.
- Swaroopa, M., Gopal, L.V., Reddy, T.K.K. and Majumdar, B., 2015. “Effect of crucible parameters on planar flow melt spinning process”. *Transactions of the Indian Institute of Metals*, Vol. 68, No. 6, pp. 1125–1129.
- Swaroopa, M., Reddy, T.K.K., Reddy, A.C. and Majumdar, B., 2017. “Flow cfd analysis of 2d transient melt flow from crucible on to the rotating wheel in planar melt spinning process”. *Materials Today: Proceedings*, Vol. 4, No. 2, pp. 2615–2623.
- Theisen, E.A. and Weinstein, S.J., 2021. “An overview of planar flow casting of thin metallic glasses and its relation to slot coating of liquid films”. *arXiv preprint arXiv:2104.09251*.
- Wang, G.X. and Matthys, E., 1991. “Modelling of rapid solidification by melt spinning: effect of heat transfer in the cooling substrate”. *Materials Science and Engineering: A*, Vol. 136, pp. 85–97.
- Wang, G.X. and Matthys, E., 1992. “Numerical modelling of phase change and heat transfer during rapid solidification processes: use of control volume integrals with element subdivision”. *International journal of heat and mass transfer*, Vol. 35, No. 1, pp. 141–153.
- Wang, G.X. and Prasad, V., 2000. “Rapid solidification: Fundamentals and modeling”. *Annual Review of Heat Transfer*, Vol. 11.
- Wang, G. and Matthys, E., 2001. “Mathematical simulation of melt flow, heat transfer and non-equilibrium solidification in planar flow casting”. *Modelling and simulation in materials science and engineering*, Vol. 10, No. 1, p. 35.
- Wang, T., Cai, S., Xu, J., Du, Y., Zhu, J., Xu, J. and Li, T., 2010. “Continuous casting mould for square steel billet optimised by solidification shrinkage simulation”. *Ironmaking & Steelmaking*, Vol. 37, No. 5, pp. 341–346.

8. RESPONSIBILITY NOTICE

The authors are solely responsible for the printed material included in this paper.